Energy level alignment at Co/AlOx/pentacene interfaces

Popinciuc, M.; Jonkman, H. T.; van Wees, B. J.

Published in:
Journal of Applied Physics

DOI:
10.1063/1.2721885

Energy level alignment at Co/AlOx/pentacene interfaces

M. Popinciuc[a] and H. T. Jonkman
Molecular Electronics, Materials Science Centre, University of Groningen, Nijenborgh 4, 9747 AG Groningen, The Netherlands

B. J. van Wees
Physics of Nanodevices, Materials Science Centre, University of Groningen, Nijenborgh 4, 9747 AG Groningen, The Netherland

(Received 17 November 2006; accepted 28 February 2007; published online 1 May 2007)

X-ray and ultraviolet photoemission spectroscopy (XPS and UPS) experiments were performed in order to study the energy level alignment and electronic structure at Co/AlOx/pentacene interfaces as a function of the aluminum oxide (AlOx) tunnel barrier thickness and the oxidation state of Co. XPS was used to determine the oxygen exposure for the optimum oxidation of 6, 8, and 10 Å thin layers of Al deposited on Co. The Fermi level (FL) position in the band gap of AlOx depends on the oxidation state of the underlying Co and on the thickness of the tunnel barrier. The energy level alignment at Co/AlOx interfaces is consistent with an interfacial dipole, its magnitude being sensitive to the oxidation of Co, and band bending phenomena in the thin AlOx tunnel barrier. UPS experiments revealed no chemical interaction at Co/AlOx/pentacene interface in contrast with hybridization effects found at Co/pentacene interface. The vacuum level of pentacene aligns with that of AlOx, following the position of AlOx energy levels with respect to FL. The hole injection barrier was found to increase with the thickness of the tunnel barrier and to decrease with the oxidation of Co at a fixed thickness of the AlOx layer. © *2007 American Institute of Physics*. [DOI: 10.1063/1.2721885]

I. INTRODUCTION

Organic spintronics is a new branch of the field of molecular electronics and deals with the injection and detection of spin polarized carriers in organic semiconductors by means of spin valve devices. Injection and detection of spins is realized by a pair of ferromagnetic electrodes, whose magnetization can be controlled independently, whereas the transport and manipulation of spins is realized in the organic semiconductor placed in between the two ferromagnets. Organic spin valve behavior was reported for sexithienyl (T6) (Ref. 1) and 8-hydroxy-quinoline aluminum (Alq3).[2] With one of the highest hole mobilities among organic semiconductors,[3] pentacene appears to be a good candidate to investigate spin transport properties. However, all electrical spin injection and detection in semiconductors (organic or inorganic) using ferromagnetic metals (such as Co) suffer from a common problem: the conductivity mismatch problem.[4] Theoretical predictions suggest that the problem can be solved by the insertion of thin tunnel barriers (e.g., aluminum oxide) in between the ferromagnetic metal and the semiconductor.[4,5] Depending on the conductivity of the organic material, tuning of the tunnel barrier resistance by tuning its thickness is generally required. Whether (and how) the tunnel barrier influences the energy levels alignment scheme at Co/AlOx/pentacene interfaces is not known. To date, there are no studies (photoemission or transport) regarding the carrier injection barriers at Co/AlOx/pentacene interfaces. The insertion of thin insulating layers of LiF in between the organic semiconductor and the metal contacts has shown to improve the performance of organic LEDs.[6–8] The effect was explained by the modification of the carrier injection barriers, information inferred from photoemission experiments.[9–13]

In this article we report on the interfacial energy level alignment between Co and pentacene in the case of insertion of a thin aluminum oxide (AlOx) tunnel barrier in between. The tunnel barriers were fabricated by depositing thin layers of Al (6, 8, and 10 Å) on Co thin films followed by thermal oxidation at room temperature. The oxidation state of Al and the oxygen exposures for which the Al layers are optimally oxidized were obtained from x-ray photoemission spectroscopy (XPS) measurements. The dependence of the binding energy (BE) and full width at half maximum (FWHM) of the Al core levels (Al 2*p* and Al 2*s*) with respect to the oxidation state of Co hint at an interface dipole sensitive to the oxidation state of the interfacial Co layer. The position of the top of the valence band of AlOx, with respect to the Fermi level, extracted from ultraviolet photoemission spectroscopy (UPS) measurements, varies as a function of the thickness of the tunnel barrier, consistent with band bending phenomena in the AlOx layer. At AlOx/pentacene interfaces the interfacial dipole is negligible. Our results show that the hole injection barrier increases with the thickness of AlOx and decreases with the oxidation of Co at a constant AlOx thickness. This enables tuning of the device performance by controlling the

[a]Electronic mail: m.popinciuc@rug.nl

thickness of the tunnel barrier. The hybridization effects present at the Co/pentacene interface are suppressed by the insertion of the AlOx tunnel barrier.

II. EXPERIMENT

The preparation of the samples and the photoemission experiments were performed *in situ* in an interconnected ultrahigh vacuum system. In the preparation chamber Co, Al, and pentacene were evaporated in background pressures $\leq 3\times10^{-9}$ mbar. Co and Al were evaporated using Radak type I cells from alumina crucibles onto oxidized silicon substrates which were liquid nitrogen cooled in order to assure a smooth surface and a closed Al layer. Pentacene, purified by vacuum sublimation and degassed before the experiments for a few hours, was deposited in a stepwise manner at room temperature from a homemade, resistively heated, glass crucible at a rate of 2.5 Å/min. All deposition thicknesses were monitored with crystal microbalances calibrated by atomic force microscopy or surface profilometry. The aluminum layers were oxidized by exposing the sample in steps to oxygen (99.5%) at room temperature. The photoemission experiments were performed at room temperature immediately after the oxygen exposure or the pentacene deposition step. The analysis chamber, base pressure of $\sim2\times10^{-10}$ mbar, is equipped with a nonmonochromatic Al $K\alpha$ x-ray source (1486.6 eV) and a nonmonochromatic He discharge lamp (UV light of 21.2 eV). The photoelectrons were analyzed with a hemispherical analyzer from Vacuum Generators. The incoming light and the analyzer are at 35° with respect to the sample surface normal. The resolution of the spectra was 1.5 eV for XPS and 0.15 eV for UPS. The UPS measurements were performed with a −4 V bias applied to the sample in order to enable the measurement of the secondary electrons cutoff.

III. RESULTS AND DISCUSSION

A. Al oxidation monitored by XPS and UPS

The tunnel barriers were derived by oxidizing 6, 8, and 10 Å Al, respectively. This was realized by evaporation of Al followed by exposure to oxygen in steps. After each exposure step XPS spectra were recorded in order to determine the optimum oxidation conditions. The oxygen exposure is expressed in langmuir (L), $1\ \mathrm{L}=1.33\times10^{-6}$ mbar s. Similar spectra were taken for all samples. A few spectra in the region of Al $2p$ and Co $2p_{1/2}$ core levels are presented in Fig. 1 for the 6 Å sample.

The energy levels of Al shift toward higher BE as the Al metal undergoes oxidation; that is, the chemical state of Al changes from Al^0 in neutral Al metal to Al^{3+} in Al_2O_3.[14] In the beginning of the oxidation process Al is present in a mixture of pure and oxidized Al. Even the as-deposited Al is partly oxidized due to the evaporation onto the liquid nitrogen cooled substrate, which increases the sticking coefficient of the residual gases. This is reflected in the width of Al $2p$ [see the bottom spectrum of Fig. 1(a)] and the presence of oxygen in the spectra (not shown). The resolution of our spectrometer did not allow clear separation of the two energy levels, one of pure Al and one of oxidized Al, so fitting of the

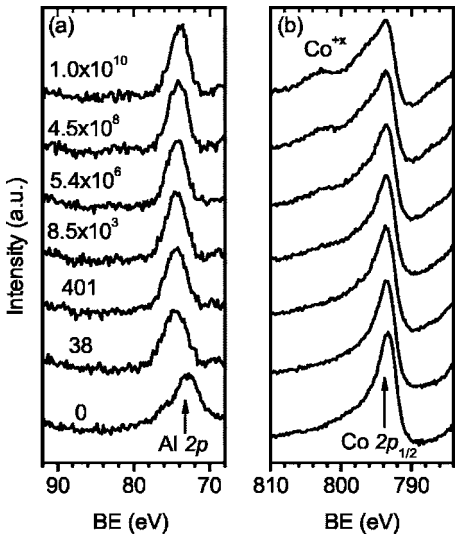

FIG. 1. A few XPS spectra of 6 Å Al metal on Co at different oxygen exposure doses (the numbers represent the total oxygen exposure expressed in langmuir and are valid for all the traces, from bottom to top). (a) Al $2p$ and (b) Co $2p_{1/2}$ regions. Note the shift of Al $2p$ energy level, the broadening of Co $2p_{1/2}$, and the appearance of oxidized cobalt levels (Co^{+x}) with increasing the oxygen exposure dose.

data was done assuming only one Gaussian function and a Shirley-type background.[14] We will show later that, in spite of this restriction, we are able to determine the optimum oxidation conditions without any doubt. The BE and FWHM of Al $2p$ and Al $2s$ energy levels were tracked as a function of total oxygen exposure; the results obtained from fitting are shown in Fig. 2 for Al $2p$ level of all samples. At low oxygen exposures the FWHM of Al $2p$ level is larger with respect to a pure or completely oxidized Al layer owing to the mixture of pure and oxidized Al. After a certain oxygen exposure the FWHM saturates, consistent with the existence of only one oxidation state of Al. Further oxygen exposure does not change the chemical state of Al; therefore, we consider that the optimum oxidation is when FWHM saturation starts, that

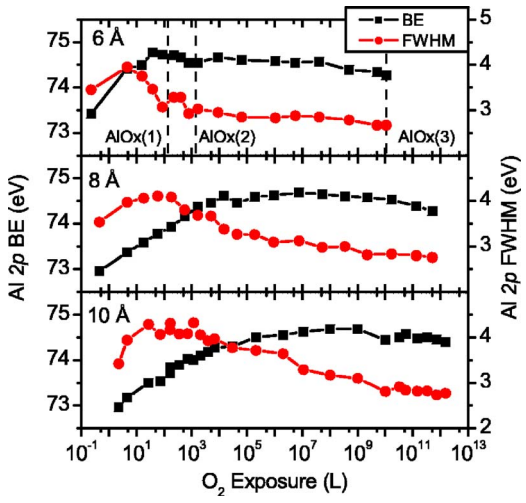

FIG. 2. The BE (squares, left axis) and FWHM (circles, right axis) of Al $2p$ energy level as a function of oxygen exposure for (from top to down) 6, 8, and 10 Å Al on Co. The vertical dashed lines represent the oxygen exposures of the three samples (6 Å Al) for which the pentacene energy level alignment was measured by UPS; see Sec. III C.

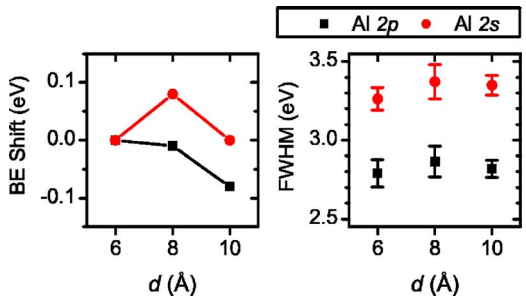

FIG. 3. (a) Binding energy shift and (b) FWHM of Al $2p$ (squares) and Al $2s$ (circles) as a function of the initial Al layer thickness.

is 140, 0.9×10^6, and 10^{10} L for the 6, 8, and 10 Å Al layers, respectively. Beyond this point, the underlying Co starts to oxidize, that is, Co $2p$ energy levels broaden as oxidized Co (Co^{+x}) energy levels develop in the spectra; see Fig. 1(b). In a separate experiment we exposed a clean Co surface to oxygen and found that Co readily oxidizes (spectra not shown). This is in contrast with the late appearance of cobalt oxide (CoOx) signs in the case the deposition of the 6 Å Al layer, suggesting a good coverage of the surface by the Al layer. Roughly, the saturation in FWHM corresponds with a peak in BE for the Al energy levels, which we interpret as an extra indication that the underlying Co layer starts to oxidize.

Figure 3 summarizes the XPS results of Al core levels of the AlOx tunnel barriers as a function of thickness of the initial Al layer (d). In all plots presented in this article we will represent the variable thickness of AlOx by the initial thickness of Al from which the tunnel barrier was derived. To obtain the thickness of the oxide barrier, d should be multiplied by a factor of $\sim$1.2 assuming the bulk densities of Al and γ-Al_2O_3. In Fig. 3(a) we present the binding energy shift of the levels with respect to d. Within less than a tenth of the experimental resolution the Al core levels have a constant binding energy. The FWHM of Al $2p$ and Al $2s$ (average values taking all the points in the saturation region) is shown in Fig. 3(b). Within the error bars, which represent the standard deviation, the FWHM is constant.

The following phenomena may take place at the Co/AlOx interface: formation of interfacial dipole, chemistry (pinning), screening effects, band bending, intermixing of Al with Co, and charging. We can exclude charging effects in XPS from the following two reasons. First, charging should broaden the energy levels with increasing the insulating layer thickness, whereas we found FWHM to be constant. Second, charging should be more severe with the appearance of the CoOx layer in between Co and AlOx and should shift the energy levels of Al toward higher energies, which is actually the opposite of what we observed. This is in agreement with previous reports which showed that charging does not occur in aluminum oxide layers thinner than 25 Å.[15,16] Intermixing of Al and Co species cannot play a major role for the following reason. Very likely, the intermixed AlOx layer would have a different FWHM compared with a pure one due to nonuniformities in the chemical environment. In fact, the FWHM should peak at the point where the probed layer consists of equal quantities of intermixed Co-AlOx and pure AlOx layers. Our data show a constant FWHM (within the

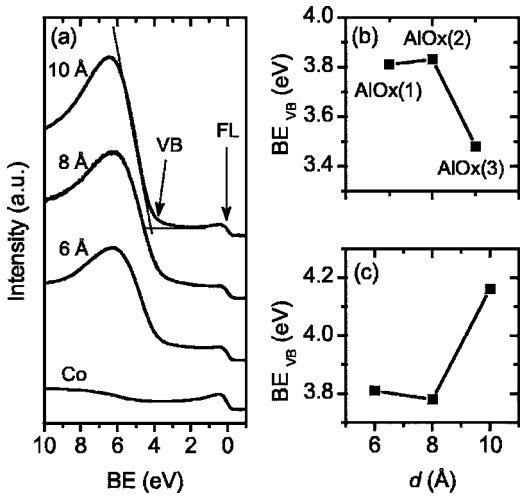

FIG. 4. (a) UPS spectra of the optimum oxidized Al layers showing the top of valence band of AlOx (VB). (b) The BE of VB (BE_{VB}) as a function of the oxidation of Co for the 6 Å sample (see the text). (c) BE of VB of AlOx as a function of initial thickness of the Al layer, d.

error bars), therefore pointing to a uniform chemical environment and to a sharp Co/AlOx interface. This is also consistent with the late appearance of Co oxidation signs, which points to a good coverage and small intermixing of Al with Co. Screening effects, due to close proximity of the Co metal, do not have a significant contribution since the Al levels shift toward lower BEs with the appearance of CoOx layer (which increases the distance between Co metal and AlOx), contrary to what would be expected if metal screening played a major role. Different FL positions with respect to a common VL of Co and AlOx lead to an interfacial dipole at Co/AlOx interface, whose magnitude is affected by the interfacial states present at Co/AlOx interface. With the appearance of a thin CoOx layer in between Co and AlOx, the nature of these interfacial states is changed and a change in the magnitude of the interfacial dipole is expected to occur, in agreement with the change (decrease) of the BE of Al core levels.

UPS spectra of optimum oxidized layers were also recorded; see Fig. 4(a). We identify the broad feature around 6.5 eV as corresponding to the valence band of aluminum oxide. The position of the top of the valence band (denoted as VB) with respect to FL as a function of oxidation state of Co and as a function of the initial Al layer thickness (d) is shown in Figs. 4(b) and 4(c). As already discussed, at the Co/AlOx interface an interfacial dipole exists and its magnitude is sensitive to the oxidation state of the underlying Co. The UPS data also show a decrease in the binding energy of the VB with oxidizing Co, in agreement with the XPS measurements (see Fig. 2). As a function of d, an increase in BE of the VB is observed in UPS in contrast with the XPS measurements. A possible explanation is a stronger differential charging in the UPS measurements, which we cannot completely exclude. However, literature data on thin aluminum oxide layers grown on various metals[16–19] showed an increase of the Al core levels binding energies with increasing the thickness of the oxide as well. Thin insulating layers of LiF deposited on metals behave similarly.[10,20] The shift to-

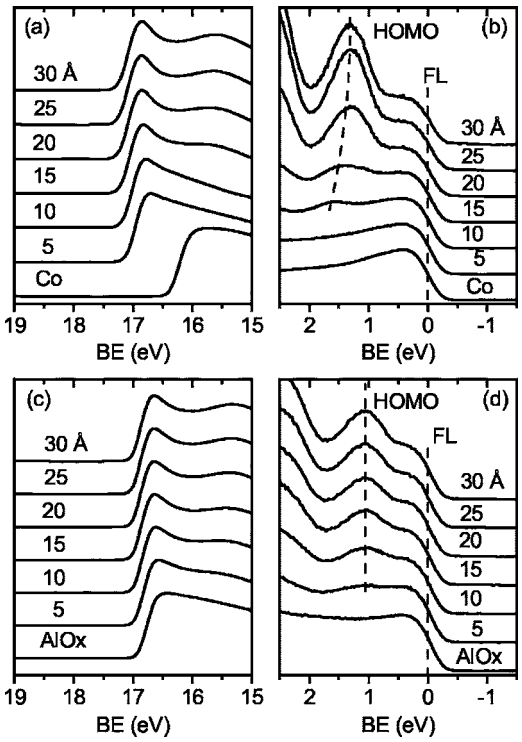

FIG. 5. (a), (b) UPS spectra of pentacene deposited on Co in the region of secondary electron cutoff and Fermi level, respectively. (c), (d) UPS spectra in the case of insertion of an optimum oxidized 6 Å Al layer between Co and pentacene. The dashed lines are a guide to the eyes and represent the FL and the evolution of HOMO level with increasing pentacene coverage.

ward higher binding energies of the energy levels of the insulating layer with increasing the insulator thickness was interpreted in most cases in terms of interfacial dipole, Schottky barrier formation, and band bending in the thin insulating layer. Taking into account the discussion of the XPS data in the previous paragraph, we believe that the energy level alignment at Co/AlOx interface is due to Schottky barrier formation and band bending in the AlOx layer.

B. Energetics of Co/AlOx/pentacene and Co/pentacene interfaces

In this section we present the results on the energetics of the Co/AlOx/pentacene interfaces. A comparison is made with the clean contact case, Co/pentacene. Pentacene was deposited in steps on the Co/AlOx substrates and UPS spectra were taken after each deposition step. In this way, we were able to map out the energy level alignment and the magnitude of the hole injection barrier as a function of pentacene thickness.

In the clean contact case between pentacene and Co, there is a high degree of interaction.[21,22] Due to hybridization of the highest molecular orbital (HOMO) of pentacene with the reactive Co 3*d* band, the BE of the HOMO level was found to be higher for the interfacial layer (submonolayer coverage of pentacene) in comparison with the two monolayer (≈30 Å) coverage situation. This is illustrated in Fig. 5(b), where we present the measured UPS spectra in the region of HOMO for a few thicknesses of pentacene. In the case of insertion of AlOx tunnel barrier in between Co and pentacene there is no chemical interaction, as the BE of the HOMO level stays approximately the same for the interfacial layer compared with a thicker film; see Fig. 5(d). Note that in the clean contact case at 5 Å pentacene coverage the HOMO level is not detectable, whereas when the tunnel barrier is inserted the HOMO level becomes visible. This behavior was consistent in all samples employing an AlOx tunnel barrier, indicating no chemical activity for Co/AlOx/pentacene system compared with Co/pentacene, in agreement with measurements on the Al/AlOx/pentacene system.[23] The hole injection barrier (the distance between leading edge of HOMO and the FL) amounts to 0.96 eV for Co/pentacene interface, whereas for Co/AlOx (6 Å)/pentacene the barrier height is 0.60 eV for the tunnel barrier derived from oxidizing 6 Å Al. At the Co/pentacene interface we found an interfacial dipole of 1.05 eV, whereas for the Co/AlOx (6 Å)/pentacene system we found an interfacial dipole of 0.67 eV at the Co/AlOx interface and vacuum level alignment at the AlOx/pentacene interface. A vacuum alignment situation was reported also for SiO_2/pentacene and LiF/pentacene interfaces.[20,24]

C. Energy level alignment at Co/AlOx/pentacene interfaces

In this section we will discuss the variation of the hole injection barrier (Δ_h) as a function of the oxidation state of the underlying Co (for the 6 Å Al samples) and as a function of the thickness of the tunnel barrier (the optimum oxidized 6, 8, and 10 Å Al layers). The energy level alignment was determined for each of the samples. All samples show a similar behavior; that is, VL alignment of pentacene with the AlOx tunnel barrier and constant HOMO binding energy with increasing thickness of pentacene, consistent with no interfacial chemical reaction between pentacene and AlOx as previously discussed.

From the organic spin valve device point of view it is of importance that Co is not oxidized at the interface with the AlOx tunnel barrier. In order to investigate to what extent the oxidation of the Co underlayer influences the hole injection barrier at Co/AlOx/pentacene interface, we prepared three similar samples (same 6 Å thickness of Al) and performed UPS measurements. The difference between the samples was the oxygen dose at which the Al layer was exposed. The oxygen exposure conditions for the three samples are indicated in Fig. 2(a) by the vertical dashed lines. The samples were denoted as: optimum oxidized AlOx(1), slightly over-oxidized AlOx(2), and over-oxidized AlOx(3) with corresponding exposures of 140, 1400, and 1×10^{10} L. For the optimum oxidized 6 Å Al sample the hole injection barrier is smaller than in the clean contact case between Co and pentacene, and decreases even more with the oxidation of Co. In Fig. 6(a) we plotted the variation of Δ_h together with the binding energy shifts of VL (at Co/AlOx interface) and Al 2*p*, Al 2*s*, for the three samples. The variable thickness samples show that Δ_h increases with the oxide thickness and amounts to 0.60, 0.65, and 0.85 eV for the 6, 8, and 10 Å Al

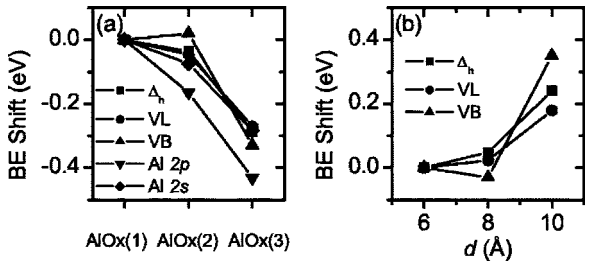

FIG. 6. (a) The variation of Δ_h, the binding energy shift of the VL at the Co/AlOx interface, the VB of AlOx, Al $2p$, and Al $2s$ for the three differently oxidized 6 Å Al samples. The hole injection barrier decreases with the oxidation of the underlying Co. (b) The variation of Δ_h and binding energy shifts of VL (at the Co/AlOx interface) and VB as a function of the initial Al layer thickness, d. The hole injection barrier increases as a function of d.

layers, respectively. In Fig. 6(b) we plotted the variation of Δ_h, BE of VL (at Co/AlOx interface), and BE of the VB of AlOx as a function of d.

The hole injection barrier, that is the HOMO level, follows the energy levels of AlOx (Al $2p$, Al $2s$, VB) in all cases. The difference between samples is the position of the FL at the interface, i.e., the work function of the substrate, determined by the oxidation of Co and/or the thickness of AlOx. A vacuum level alignment situation (the Schottky-Mott limit) was found at all interfaces between Co/AlOx substrates and pentacene; the band alignment scheme is not determined by the position of the FL in the band gap of the aluminum oxide tunnel barrier. In view of recent efforts to describe the interface energetics of organic semiconductors with various substrates,[25,26] the Co/AlOx/pentacene interfaces are characterized as weakly interacting. The charge transfer between Co and pentacene through the (transparent) AlOx barrier, due to the electrochemical potential equilibration, does not have a major contribution in determining the energy levels alignment at the Co/AlOx/pentacene interface, i.e., the interfacial slope parameter is unity.

IV. CONCLUSIONS

The evolution of Al energy levels, in thin AlOx tunnel barriers, as a function of the oxidation of the underlying Co and as a function of the aluminum oxide thickness, was interpreted as due to a combination of two factors: interfacial dipole and band bending. The energetics of Co/AlOx interface determines the band offsets and the magnitude of the interfacial dipole, which decreases with the oxidation of Co. The vacuum levels of pentacene and Co/AlOx substrates were found to align, a situation which corresponds to the Schottky-Mott limit. Charge transfer through the thin tunnel barrier (due to electrochemical potential equilibration) does not a play a significant role in determining the energy level alignment scheme. The hole injection barrier decreases with the oxidation of the bottom Co layer and increases with the thickness of aluminum oxide, following the shift of Al energy levels with respect to FL. This demonstrates that the carrier injection barriers (holes and electrons) can be tuned by varying the oxide barrier thickness. Moreover, we showed that with the insertion of a thin AlOx tunnel barrier (the 6 Å Al case) the hole injection barrier decreases by ~0.35 eV compared with the clean contact case, and an improvement in the efficiency of injecting holes is expected to occur in electrical devices. The contact resistance of Co/AlOx/pentacene devices is expected to increase with the tunnel barrier thickness due to the following reasons. First, as the aluminum oxide becomes thicker, fewer carriers are able to tunnel through; second, at the same time, the carriers experience a higher injection barrier. Since the magnitude of the hole injection barrier is important in the modeling of the spin valves, the information gained from our experiments will help to successfully model and design organic spin valves employing Co, AlOx tunnel barriers and pentacene.

ACKNOWLEDGMENTS

M.P. wishes to acknowledge A. Heeres for technical support and L. H. Tan for assistance is some of the experiments. Financial support was given by the Dutch Foundation for Fundamental Research on Matter (FOM) and Materials Science Centre (MSC) Groningen, The Netherlands.

[1] V. Dediu, M. Murgia, F. C. Matacota, C. Taliani, and S. Barbanera, Solid State Commun. **122**, 181 (2002).
[2] Z. H. Xiong, D. Wu, Z. V. Vardeny, and J. Shi, Nature **427**, 821 (2004).
[3] O. D. Jurchescu, J. Baas, and T. T. M. Palstra, Appl. Phys. Lett. **84**, 3061 (2004).
[4] G. Schmidt, D. Ferrand, L. W. Molenkamp, A. T. Filip, and B. J. van Wees, Phys. Rev. B **62**, R4790 (2000).
[5] A. Fert and H. Jaffres, Phys. Rev. B **64**, 184420 (2001).
[6] L. S. Hung, C. W. Tang, and M. G. Mason, Appl. Phys. Lett. **70**, 152 (1997).
[7] G. E. Jabbour, Y. Kawabe, S. E. Shaheen, J. F. Wang, M. M. Morrell, B. Kippelen, and N. Peyghambarian, Appl. Phys. Lett. **71**, 1762 (1997).
[8] S. E. Shaheen, G. E. Jabbour, M. M. Morrell, Y. Kawabe, B. Kippelen, M.-F. Nabor, R. Schlaf, E. A. Mash, and N. R. Armstrong, J. Appl. Phys. **84**, 2324 (1998).
[9] T. Mori, H. Fujikawa, S. Tokito, and Y. Taga, Appl. Phys. Lett. **73**, 2763 (1998).
[10] R. Schlaf, B. A. Parkinson, P. A. Lee, K. V. Nebesny, G. Jabbour, B. Kippelen, N. Peyghambarian, and N. R. Armstrong, J. Appl. Phys. **84**, 6729 (1998).
[11] Q. T. Le, L. Yan, Y. Gao, M. G. Mason, D. J. Giesen, and C. W. Tang, J. Appl. Phys. **87**, 375 (2000).
[12] G. Greczynski, F. Fahlman, and W. R. Salaneck, J. Chem. Phys. **113**, 2407 (2000).
[13] M. G. Mason, C. W. Tang, L.-S. Hung, P. Raychaudhuri, J. Madathil, D. J. Giesen, L. Yan, Q. T. Le, Y. Gao, S.-T. Lee *et al.*, J. Appl. Phys. **89**, 2756 (2001).
[14] S. Hüfner, *Photoelectron Spectroscopy* (Springer-Verlag, Berlin, 1995).
[15] T. L. Barr, J. Vac. Sci. Technol. A **7**, 1677 (1989).
[16] T. L. Barr, S. Seal, L. M. Chen, and C. C. Kao, Thin Solid Films **253**, 277 (1994).
[17] Y. Wu, E. Garfunkel, T. E. Madey, and N. D. Shinn, Surf. Sci. **336**, 123 (1995).
[18] Y. Wu, E. Garfunkel, and T. E. Madey, Surf. Sci. **365**, 337 (1996).
[19] Y. Yamauchi, M. Yoshitake, and W. Song, Appl. Surf. Sci. **237**, 363 (2004).
[20] N. J. Watkins and Y. Gao, J. Appl. Phys. **94**, 1289 (2003).
[21] M. Popinciuc, H. T. Jonkman, and B. J. van Wees, Appl. Surf. Sci. **100**, 093714 (2006).
[22] M. V. Tiba, W. J. M. de Jonge, B. Koopmans, and H. T. Jonkman, Appl. Surf. Sci. **100**, 093707 (2006).
[23] N. J. Watkins, S. Zorba, and Y. Gao, J. Appl. Phys. **96**, 425 (2004).
[24] N. J. Watkins and Y. Gao, J. Appl. Phys. **94**, 5782 (2003).
[25] H. Vázquez, R. Oszwaldowski, P. Pou, J. Ortega, R. Pérez, F. Flores, and A. Kahn, Europhys. Lett. **65**, 802 (2004).
[26] C. Tengstedt, W. Osikowicz, W. R. Salaneck, I. D. Parker, C.-H. Hsu, and M. Fahlman, Appl. Phys. Lett. **88**, 053502 (2006).